A simple RLCC-diode-opamp chaotic oscillator

Article *in* International Journal of Bifurcation and Chaos · December 2014

DOI: 10.1142/S0218127414501557

CITATIONS
13

READS
923

3 authors:

Wimol San-Um
Thai-Nichi Institute of Technology
85 PUBLICATIONS **237** CITATIONS
SEE PROFILE

Bandhit Suksiri
Roland DG Corporation
28 PUBLICATIONS **40** CITATIONS
SEE PROFILE

Patinya Ketthong
Thai-Nichi Institute of Technology
14 PUBLICATIONS **48** CITATIONS
SEE PROFILE

International Journal of Bifurcation and Chaos, Vol. 24, No. 12 (2014) 1450155 (8 pages)

DOI: 10.1142/S0218127414501557

A Simple RLCC-Diode-Opamp Chaotic Oscillator

Wimol San-Um*, Bandhit Suksiri† and Patinya Ketthong‡
Intelligent Electronic System (IES) Research Laboratory,
Faculty of Engineering, Thai-Nichi Institute of Technology (TNI),
1771/1 Pattanakarn Rd., Suanluang, Bangkok 10250, Thailand
**wimol@tni.ac.th*
†*bandhit.tni@gmail.com*
‡*patinya.ket@gmail.com*

Received December 6, 2013; Revised April 8, 2014

This paper presents a simple autonomous chaotic oscillator. The design method is primarily based on a linear oscillator constructed by a closed loop connection of two building blocks, i.e. an inverting active integrator and a passive second-order LC integrator. A diode is inserted in parallel to the two building blocks for inducing chaos. The mathematical model reveals a set of three-dimensional ordinary differential equations, containing seven terms with four constants and an exponential nonlinearity. The dynamics properties are investigated in terms of an equilibrium point, Jacobian matrix, chaotic attractors, bifurcation, Lyapunov exponents, and chaotic waveforms in time domain. The proposed chaotic oscillator potentially exhibits complex dynamical behaviors through the utilization of only six minimal electronic components.

Keywords: Chaotic oscillator; diode nonlinearity.

1. Introduction

Developments of chaotic oscillators have received considerable interest due to possible applications in science and engineering such as in secure communications or in cryptography. A search on simple and robust stand-alone chaotic oscillators with minimal number of physical components has therefore been made continuously in the past decades in order to attain simplicity in practical circuit implementations. A category of chaotic oscillators that exclusively employ a set of common electronic components, i.e. a compound capacitor (C) and inductor (L) network, a resistor (R), an opamp, and a diode utilized as a nonlinear device, has been of particular interest since circuit realizations can be made possible through a modification of classical sinusoidal oscillators with minimal components.

An existing chaotic oscillator in such a category was invented by *Leon Chua* in 1983 commonly known as Chua's circuit [Chua *et al.*, 1989], which essentially exploits a CLC-network and a nonlinear negative resistance. A number of modified Chua's circuits with distinctive nonlinear dynamics have extensively been reported, including, for example, a one-diode circuit [Saito, 1989], genesis of Chua's circuit [Chua, 1992], and a modified Chua's diode nonlinearity [Zeraoulia & Sprott, 2010]. Alternatively, Elwakil and Kennedy [2000a] have suggested a semi-systematic methodology for chaotic oscillator designs based on classical sinusoidal oscillators. This methodology has led to several developments of simple chaotic oscillators based on a current feedback opamp [Elwakil & Kennedy, 2000b], a noninverting amplifier and a series LCR resonance

*Author for correspondence

[Mykolaitis *et al.*, 2005; Tamasevicius *et al.*, 2005], jerk dynamics [Sprott, 2011], and a biquad filter [Banerjee *et al.*, 2010; Banerjee *et al.*, 2012]. It can be noticed that these chaotic oscillators utilize a noninverting amplifier as a major active building block, and therefore the circuit essentially requires more than six components since other three energy storage elements and a single nonlinear device are required for chaos.

Recently, Piper and Sprott [2010] have proposed a seven-component chaotic oscillator designated as a "CLC circuit" through a closed loop connection of an inverting active integrator, a passive second-order LC integrator and a comparator with inherent signum nonlinearity. Srisuchinwong and Munmuangsaen [2012] ultimately presented a set of four simple current tunable chaotic oscillators using floating or virtually-grounded diodes, each of which comprises only six minimal components. Common features of chaotic oscillators proposed in [Piper & Sprott, 2010; Srisuchinwong & Munmuangsaen, 2012] are the realization of an inverting active integrator as a major active building block, and the nonlinear devices are inserted in series to other blocks in a closed loop.

This paper presents a simple autonomous RLCC-Diode-Opamp chaotic oscillator with only six electronic components. The design method is primarily based on a linear oscillator constructed by a closed loop connection of two building blocks, i.e. an inverting active integrator and a passive second-order LC integrator. In contrast to other design approaches, a diode is inserted in parallel to the two building blocks, and therefore an opamp with high gain or a current source is no longer required. The mathematical model reveals a three-dimensional ordinary differential system, containing seven terms with four constants and a single exponential nonlinearity. The dynamics properties are investigated in terms of an equilibrium point, Jacobian matrix, attractor, bifurcation, Lyapunov exponents, and chaotic waveforms in time domain.

2. Circuit Descriptions and Analysis

Figure 1 shows the circuit diagram of the proposed chaotic oscillator. The circuit consists of six components, including a single operational amplifier (A), an inductor (L), a resistor (R), two capacitors (C_1 and C_2), and a diode. The circuit design is primarily based on a simple linear oscillator constructed by a positive feedback loop of two main building blocks, i.e. a second-order passive integrator formed by L and C_1, and an active integrator formed by the opamp, R and C_2. The floating diode, which is a simple nonlinear device with an inherent exponential function, is inserted in parallel to those of two building blocks in order to induce the circuit for chaos. Nonlinear dynamics can be changed through the bifurcation resistor R.

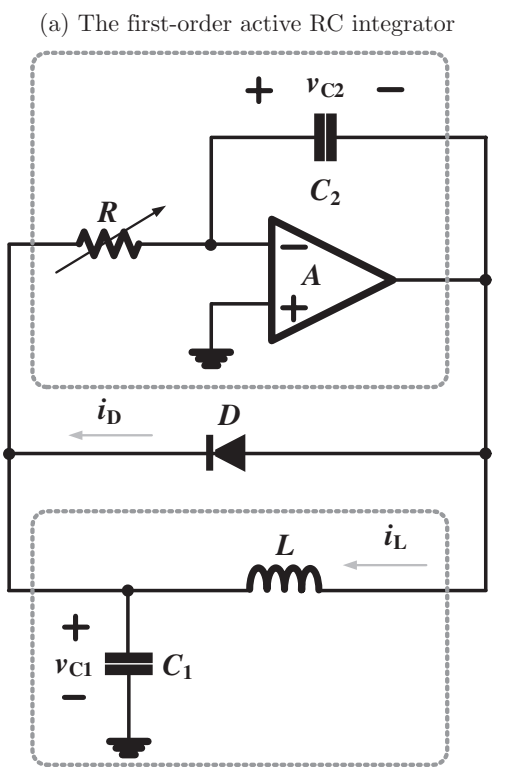

Fig. 1. The circuit diagram of the proposed RLCC-Diode-Opamp chaotic oscillator.

In order to formulate a mathematical model of the circuit in Fig. 1, the voltages across capacitors C_1 and C_2 are defined as v_{C1} and v_{C2}, respectively. The currents flowing through the inductor and the diode are defined as i_L and i_D, respectively. The parasitic series resistance of the inductor defined as R_L is also involved. Applying Kirchhoff's law to classical circuit analysis reveals a mathematical model in a set of three first-order autonomous differential equations as follows:

$$\frac{dv_{C1}}{dt} = -\frac{v_{C1}}{RC_1} + \frac{i_L}{C_1} + \frac{i_D}{C_1},$$

$$\frac{dv_{C2}}{dt} = \frac{v_{C1}}{RC_2},$$

$$\frac{di_L}{dt} = -\frac{v_{C1}}{L} - \frac{v_{C2}}{L} - \frac{R_L i_L}{L}. \tag{1}$$

The nonlinear diode current i_D in (1) is given by

$$i_D = Is\left(\exp\left(\frac{-v_{C2} - v_{C1}}{nV_T}\right) - 1\right) \tag{2}$$

where I_S is a reverse bias saturation current, n is a diode ideality factor, V_T is a thermal voltage. In order to express the dimensionless form of (1), the normalized state variables (X, Y, Z) and the system constants (A, B, C) are given by

$$\begin{bmatrix} \dot{X} & X & A \\ \dot{Y} & Y & B \\ \dot{Z} & Z & C \end{bmatrix} = \begin{bmatrix} \dfrac{dX}{d\tau} & \dfrac{v_{C1}}{nV_T} & \dfrac{\tau_L}{\tau_1} \\ \dfrac{dY}{d\tau} & \dfrac{v_{C2}}{nV_T} & \dfrac{\tau_L}{\tau_3} \\ \dfrac{dZ}{d\tau} & \dfrac{i_L R_L}{nV_T} & \dfrac{\tau_L}{\tau_2} \end{bmatrix} \tag{3}$$

where time constants are defined as $\tau = t/\tau_L$, $\tau_L = L/R_L$, $\tau_1 = RC_1$, $\tau_2 = RC_2$, and $\tau_3 = R_L C_1$. In addition to (3), the constant D is also expressed as $D = R_L \tau_L I_S / nV_T \tau_3$. Accordingly, the dimensionless form of the set of differential equations in (1) is given by

$$\begin{bmatrix} \dot{X} \\ \dot{Y} \\ \dot{Z} \end{bmatrix} = \begin{bmatrix} -A & 0 & B \\ C & 0 & 0 \\ -1 & -1 & -1 \end{bmatrix} \begin{bmatrix} X \\ Y \\ Z \end{bmatrix} + \begin{bmatrix} D(\exp(-Y - X) - 1) \\ 0 \\ 0 \end{bmatrix}. \tag{4}$$

It is seen in (4) that the system algebraically contains seven terms with four constants and one exponential nonlinearity. Dynamic behaviors can be changed by tuning the resistor R, which directly changes the time constants τ_1 and τ_2 that subsequently affects the values of the constants A and C in equations $\dot{X}$ and $\dot{Y}$, respectively. In other words, the change in resistor R has no effects on the diode equation. Upon setting (4) equal to zero, a single equilibrium point is found at $P = (0, -q, q)$ where q is a solution of the nonlinear equation

$$Z + \frac{D\exp(Z)}{B} = 0. \tag{5}$$

Such a solution q can be found through numerical methods. The Jacobian matrix (J) of (4) at the equilibrium point P can be defined as follows:

$$J = \begin{bmatrix} -A - D\exp(-q) & -D\exp(-q) & B \\ C & 0 & 0 \\ -1 & -1 & -1 \end{bmatrix}. \tag{6}$$

Applying $|\lambda I - J| = 0$ where λ is an eigenvalue and I is an identity matrix, the characteristic equation of (6) can be found as follows;

$$\begin{aligned} \lambda^3 &+ ((1 + A) + D\exp(q))\lambda^2 \\ &+ ((A + B + BC) + (1 + C)D\exp(q))\lambda \\ &+ (CD\exp(q)) = 0. \end{aligned} \tag{7}$$

The resulting eigenvalues obtained from (7), which determine system stability, depend on system constants, the diode reverse bias saturation current, and the term $\exp(q)$. It can be concluded all passive components mutually determine the system dynamical behaviors.

3. Numerical Simulations

The dynamics properties of the system (4) were numerically simulated in MATLAB using Adams–Bashforth–Moulton method with time step size of 1×10^{-6}. Initial conditions were set at (0.1, 0, 0), which is a point that is not an equilibrium point and is close to the origin. Electronic components are $C_1 = 1\,\mu$F, $C_2 = 10\,$nF, and $L = 22\,$mH with $R_L = 98\,\Omega$. The diode is 1N4148 using Spice parameters $I_S = 2.682 \times 10^{-9}\,$A, $V_T = 25.85 \times 10^{-3}\,$V, and $n = 1.96$.

Initially, qualitative and quantitative measures of chaos using bifurcation diagram and Lyapunov Exponent (LE) spectrum, respectively, were performed over an appropriate resistor range between $0\,\Omega$ to $300\,\Omega$. Figure 2(a) shows the bifurcation diagram of $v_{c1,\max}$ over the region of the tuning resistance R in the range $0\,\Omega$ to $30\,\Omega$, apparently showing a period doubling to chaos. In addition, Fig. 2(b) shows the bifurcation diagram of $v_{c1,\max}$ over the whole region of tuning resistance R in the range between $0\,\Omega$ to $300\,\Omega$. Figure 3 shows the positive LE spectrum over the whole region of tuning resistance R in the range between $0\,\Omega$ to $300\,\Omega$. The maximum positive LE value of approximately 0.158 was found at $R = 30\,\Omega$, which is particularly employed for verifications of chaos dynamics.

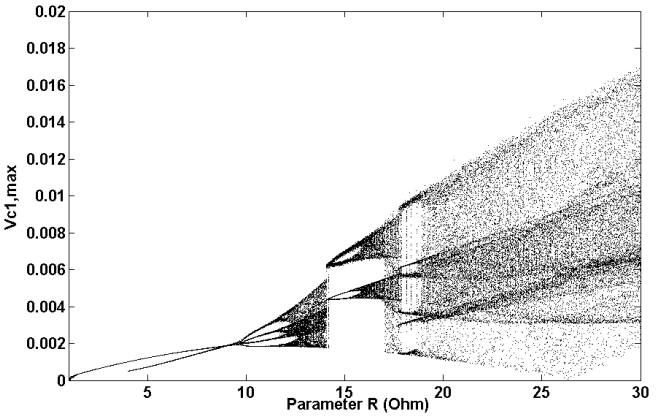

(a)

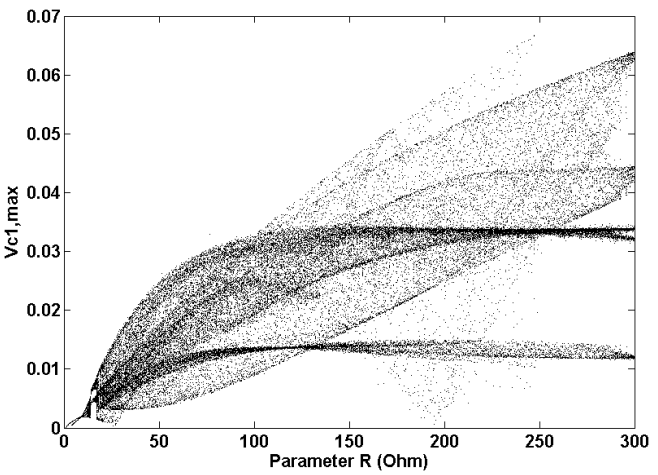

(b)

Fig. 2. The bifurcation diagrams: (a) the tuning resistance R in the range between $0\,\Omega$ to $30\,\Omega$, showing period doubling to chaos and (b) the tuning resistance R in the range between $0\,\Omega$ to $300\,\Omega$.

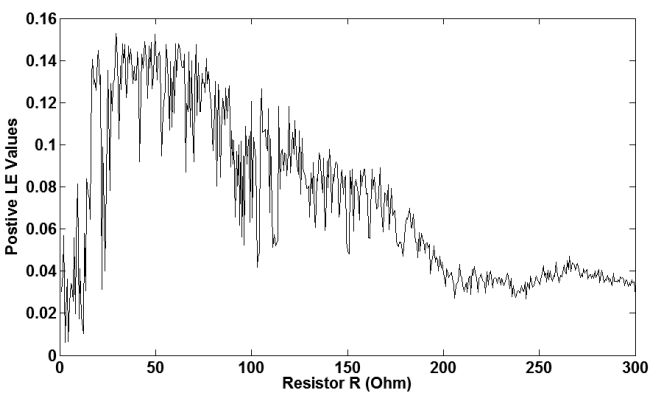

Fig. 3. The positive Lyapunov exponent spectrum over the tuning resistance R in the range between $0\,\Omega$ to $300\,\Omega$.

Table 1. Summary of numerical values of time constants and system constants.

(a) Time Constants	Values (s)	(b) System Constants	Values
τ_L	2.25×10^{-4}	A	448.98
τ_1	5×10^{-1}	B	229.07
τ_2	5×10^{-5}	C	4.49
τ_3	9.8×10^{-7}	D	1.19×10^{-5}

Table 1 summarizes the numerical values of time constants and system constants. With reference to Table 1, the equilibrium point is $P = (0, 5.1876 \times 10^{-6}, -5.1876 \times 10^{-6})$, which is very close to the origin. The Jacobian matrix is

$$J = \begin{bmatrix} -4.6769 & 0 & 2.2907 \\ 467.6871 & 0 & 0 \\ -1 & -1 & -1 \end{bmatrix}. \tag{8}$$

The characteristic equation described in (7) with numerical coefficients is

$$\lambda^3 + 5.6769\lambda^2 + 6.9732\lambda + 1.0713 \times 10^3 = 0. \tag{9}$$

As a result of (9), the three eigenvalues are

$$\begin{bmatrix} \lambda_1 \\ \lambda_2 \\ \lambda_3 \end{bmatrix} = \begin{bmatrix} -12.2486 \\ 3.2858 - 8.7561i \\ 3.2858 + 8.7561i \end{bmatrix}. \tag{10}$$

It is apparently seen in (10) that the form of eigenvalues is a set of a single negative real number and a complex conjugate with positive real number. The system therefore exhibits the spiral saddle with index two.

4. Experimental Results

Experimental results have been conducted using discrete electronic components. The measured values are $C_1 = 1.062\,\mu$F, $C_2 = 10\,$nF, and $L = 21.6\,$mH with $R_L = 98\,\Omega$. The opamp is μA741 with a dual power supply of $\pm 12\,$V. The diode is 1N4148. The $10\,$kΩ potentiometer was realized for tuning chaos dynamics. Figure 4 shows experimental waveforms of v_{C1} and the inverted v_{C2} measured from oscilloscope traces where peak-to-peak differences are $130\,$mV and $2.80\,$V, respectively. Since

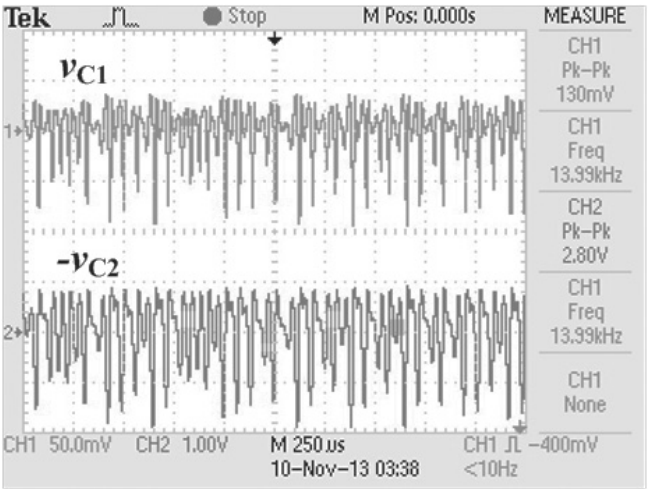

Fig. 4. Chaotic waveforms of v_{C1} and the inverted v_{C2} in time domain obtained from oscilloscope traces using $R = 50\,\Omega$.

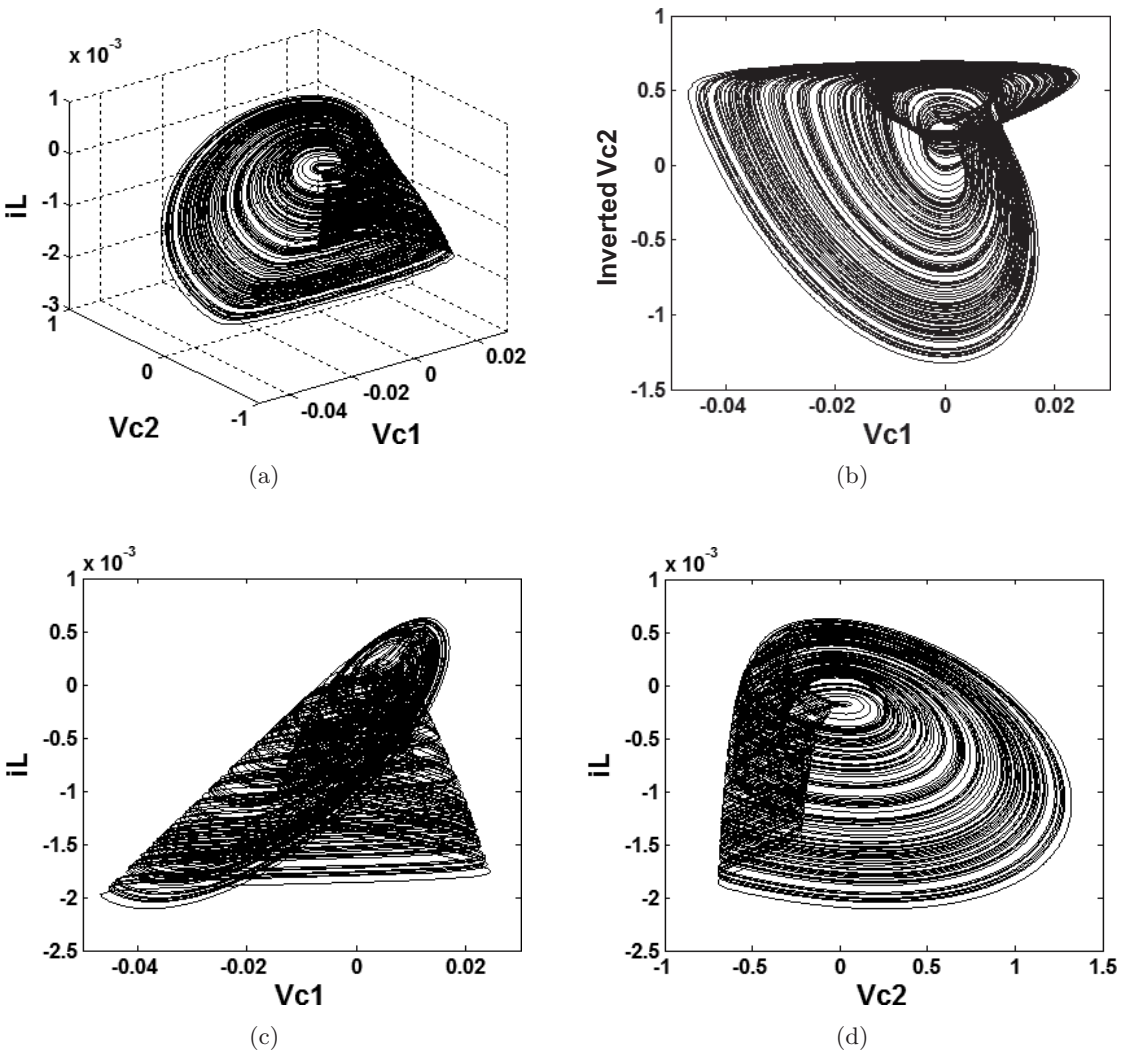

Fig. 5. Demonstrations of numerical phase-space trajectories of v_{C1}, v_{C2}, and i_L at $R = 50\,\Omega$: (a) a three-dimensional view, (b) a v_{C1}–inverted v_{C2} plane, (c) a v_{C1}–i_L plane and (d) a v_{C2}–i_L plane.

v_{C2} is the voltage across C_2 and therefore the voltage at the opamp output node with reference to ground, i.e. the inverted v_{C2}, is demonstrated. It is seen in Fig. 4 that both amplitude and frequency of the waveforms in time domain are random, i.e. the waveform is chaotic.

Figure 5 demonstrates numerical phase-space trajectories of v_{C1}, v_{C2}, and i_L, involving (a) a three-dimensional view, (b) a (v_{C1}, inverted v_{C2}) plane, (c) a (v_{C1}, i_L) plane, and (d) a (v_{C2}, i_L) plane. The attractor in three-dimensional view resembles a spiral single-scroll-like topology, which is relatively related to existing attractors that utilize a diode as a nonlinear device.

Figure 6 shows the attractor forming mechanisms obtained from numerical simulations on (v_{C1}, inverted v_{C2}) plane by varying the tuning resistor R, involving (a) period-1 using $R = 9.5\,\Omega$, (b) period-2 using $R = 12\,\Omega$, (c) period-4 using $R = 16\,\Omega$ and (d) chaotic attractor using $R = 50\,\Omega$. Figure 7 also shows attractor forming mechanisms measured from oscilloscope traces on (v_{C1}, inverted v_{C2}) plane by varying the tuning resistor R, involving (a) period-1 using $R = 9.5\,\Omega$, (b) period-2 using $R = 12\,\Omega$, (c) period-4 using $R = 16\,\Omega$ and (d) chaotic attractor using $R = 50\,\Omega$. The forming mechanisms of attractors are consistent with the bifurcation diagram in Fig. 2 and the LE spectrum

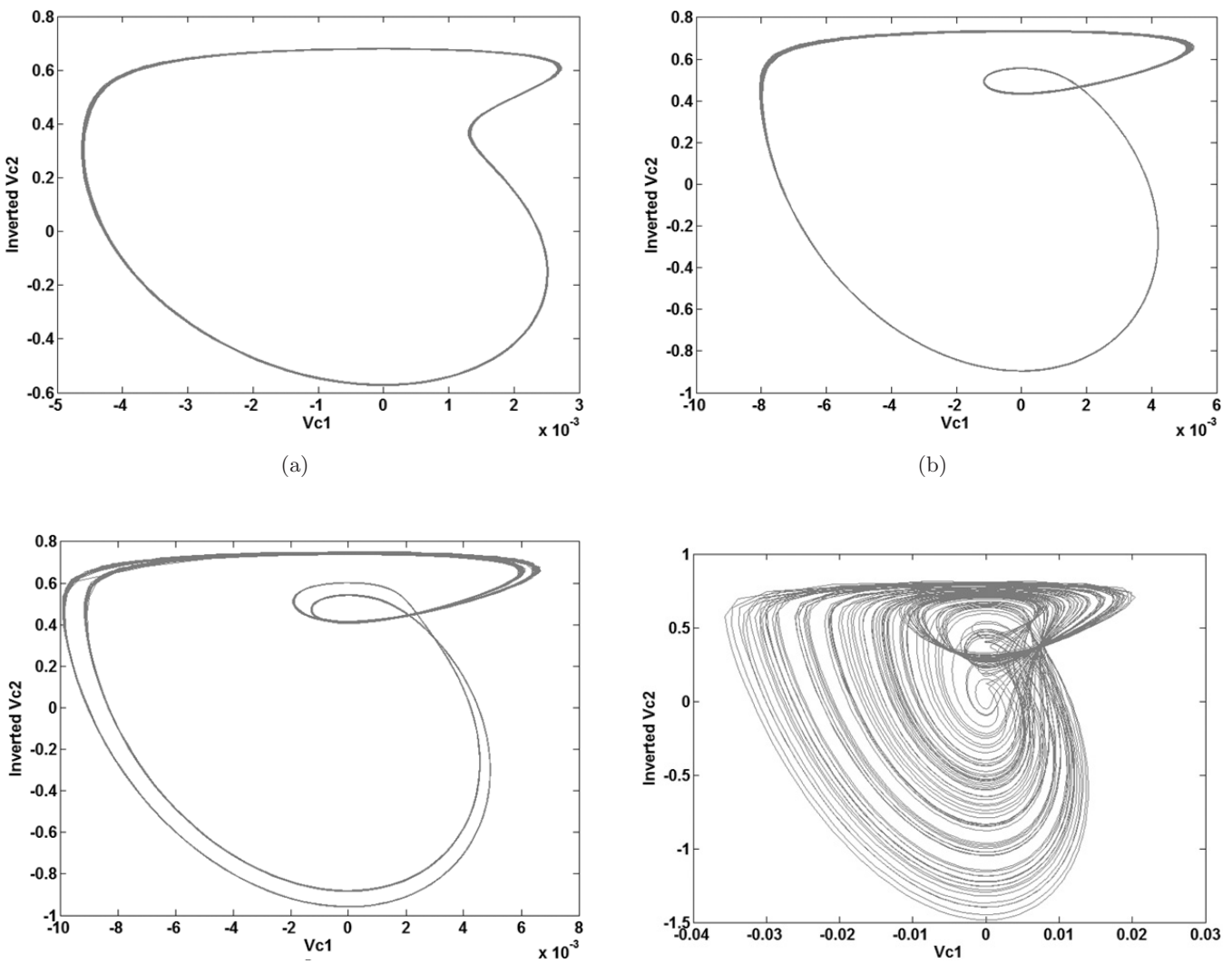

Fig. 6. Attractor forming mechanisms obtained from numerical simulations on (v_{C1}, inverted v_{C2}) plane by varying the tuning resistor R, involving (a) period-1 using $R = 9.5\,\Omega$, (b) period-2 using $R = 12\,\Omega$, (c) period-4 using $R = 16\,\Omega$ and (d) chaotic attractor using $R = 50\,\Omega$.

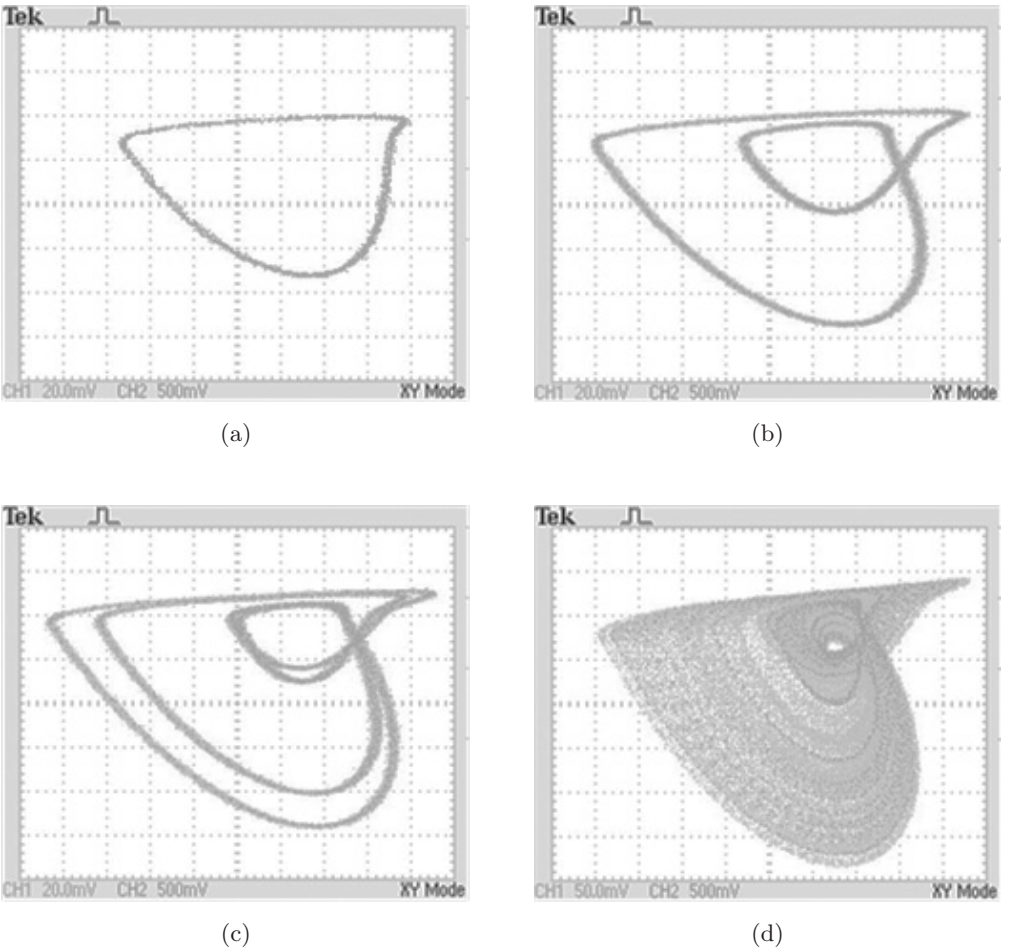

Fig. 7. Attractor forming mechanisms measured from oscilloscope traces on (v_{C1}, inverted v_{C2}) plane by varying the tuning resistor R, involving (a) period-1 using $R = 9.5\,\Omega$, (b) period-2 using $R = 12\,\Omega$, (c) period-4 using $R = 16\,\Omega$ and (d) chaotic attractor using $R = 50\,\Omega$.

depicted in Fig. 3. In addition, the chaotic attractor using $R = 50\,\Omega$ is similar to the numerically simulated attractor in Fig. 5(b). It can be concluded that the results from numerical simulations and experiments are highly consistent.

5. Conclusions

This paper has presented a new simple autonomous chaotic oscillator based on an insertion of a diode in parallel to a linear oscillator constructed by a closed loop connection of an inverting active RC integrator and a passive second-order LC integrator. The resulting mathematical model is a set of three-dimensional ordinary differential equations, containing seven terms with four constants and an exponential nonlinearity. Numerical and experimental results under a particular set of electronic components are consistent as illustrated by time-domain waveforms and phase-space trajectories. The circuit has potentially demonstrated complex chaotic behaviors through the use of only six common electronic components and hence the name "RLCC-Diode-Opamp Chaotic Oscillator".

Acknowledgments

This work is financially supported by Research and Academic Services Division, Thai-Nichi Institute of Technology through the research Grant No. 1112/A002.

References

Banerjee, T., Karmakar, B. & Sarkar, B. C. [2010] "Single amplifier biquad based autonomous electronic oscillators for chaos generation," *Nonlin. Dyn.* **62**, 859–866.

Banerjee, T., Karmakar, B. & Sarkar, B. C. [2012] "Chaotic electronic oscillator from single amplifier

biquad," *AEU-Int. J. Electron. Commun.* **66**, 593–597.

Chua, L. O., Komuro, M. & Matsumoto, T. [1989] "The double scroll family," *IEEE Trans. Circuits Syst.-I*: *Reg. Papers* **33**, 1072–1118.

Chua, L. O. [1992] "The genesis of Chua's circuit," *Archiv fir Elektronik und Iibertragungs Technik* **46**, 250–257.

Elwakil, A. S. & Kennedy, M. P. [2000a] "A semi-systematic procedure for producing chaos from sinusoidal oscillators using diode-inductor and FET-capacitor composites," *IEEE Trans. Circuits Syst.-I*: *Fund. Th. Appl.* **47**, 582–590.

Elwakil, A. S. & Kennedy, M. P. [2000b] "Chaotic oscillators derived from sinusoidal oscillators based on the current feedback opamp," *Anal. Integr. Circuits Sign. Process.* **24**, 239–251.

Mykolaitis, G., Tamasevicius, A., Bumeliene, S., Namajunas, A., Pyragas, K. & Pyragas, V. [2005] "Application of ultrafast Schottky diodes to high megahertz chaotic oscillators," *Acta Phys. Polon. A* **107**, 365–368.

Piper, J. R. & Sprott, J. C. [2010] "Simple autonomous chaotic circuits," *IEEE Trans. Circuits Syst.-II*: *Exp. Briefs* **57**, 730–734.

Saito, T. [1989] "A chaotic circuit family including one diode," *Electron. Commun. Japan* (*Part III*: *Fund. Electron. Sci.*) **72**, 52–59.

Sprott, J. C. [2011] "A new chaotic jerk circuit," *IEEE Trans. Circuits Syst.-II*: *Exp. Briefs* **58**, 240–243.

Srisuchinwong, B. & Munmuangsaen, B. [2012] "Four current-tunable chaotic oscillators in set of two diode-reversible pairs," *Electron. Lett.* **48**, 1051–1053.

Tamasevicius, A., Mykolaitis, G., Pyragas, V. & Pyragas, K. [2005] "A simple chaotic oscillator for educational purposes," *Eur. J. Phys.* **26**, 61–63.

Zeraoulia, E. & Sprott, J. C. [2010] "Generating 3-scroll attractors from one Chua's circuit," *Int. J. Bifurcation and Chaos* **20**, 135–144.